Rapid Communications

Fragile magnetic ground state of a spin-$\frac{1}{2}$ metal-organic kagome lattice

A. Jain,[1,2] S. M. Yusuf,[1,2,*] P. Kanoo,[3,†] S. K. Dhar,[4] and Tapas Kumar Maji[3]

[1]*Solid State Physics Division, Bhabha Atomic Research Centre, Mumbai 400 085, India*

[2]*Homi Bhabha National Institute, Anushaktinagar, Mumbai 400 094, India*

[3]*Chemistry and Physics of Materials Unit, Jawaharlal Nehru Centre for Advanced Scientific Research, Jakkur, Bangalore 560 064, India*

[4]*Department of Condensed Matter Physics and Materials Science, Tata Institute of Fundamental Research, Homi Bhabha Road, Colaba, Mumbai 400 005, India*

(Received 22 January 2019; revised manuscript received 2 April 2020; accepted 13 April 2020; published 30 April 2020)

We report thermodynamic and neutron diffraction measurements on a $S = 1/2$ metal-organic kagome compound $\{[Cu_3(CO_3)_2(bpe)_3]\cdot 2ClO_4\}_n$ [bpe=1,2-bis(4-pyridyl)ethane] with a Curie-Weiss temperature of $\sim -2.9 \pm 0.9$ K. The dc and ac magnetization measurements as well as neutron diffraction study show no long-range magnetic order down to 1.5 K. The temperature dependence of specific heat also shows no signature of long-range magnetic order down to 86 mK, as expected for an ideal Heisenberg kagome lattice with a nearest-neighbor antiferromagnetic exchange interaction. The frequency-independent flattening behavior observed in the real part of the ac susceptibility in a zero applied magnetic field below ~6 K rules out the presence of a spin glass state and indicates a slowing down of the spin dynamics at low temperatures. Our results suggest that strong quantum fluctuations enhanced by geometrical frustration suppress the long-range magnetic order and a ground state with quasistatic short-range canted antiferromagnetic-type order is realized in the $\{[Cu_3(CO_3)_2(bpe)_3]\cdot 2ClO_4\}_n$ [bpe=1,2-bis(4-pyridyl)ethane]. The ground state is fragile against external magnetic fields. An applied magnetic field of 125 Oe (and higher) induces ferromagneticlike spin-spin correlations.

DOI: 10.1103/PhysRevB.101.140413

Novel quantum states in a condensed matter system involving electronic spins arise when spins are arranged on a nonbipartite lattice and the magnetic exchange interaction among them is antiferromagnetic (AFM) [1–5]. The presence of competing exchange interactions in these systems may give rise to a novel fluidlike state called the "spin-liquid" state [1,2]. The experimental and theoretical investigations of such systems have attracted a great attention after the proposed resonating-valence-bond (RVB) state in the $S = 1/2$ triangular lattice Heisenberg antiferromagnets by Anderson [6]. It is now widely believed that a $S = 1/2$ kagome-lattice Heisenberg antiferromagnet, where spins form a two-dimensional (2D) network of corner-sharing triangles, is an ideal system to look for the exotic spin-liquid state [7–10]. The kagome network of corner-sharing triangles in these systems is highly frustrated, which gives rise to a large macroscopic ground-state degeneracy. Due to an extensive ground-state degeneracy, small perturbations, such as chemical doping, magnetic field, and pressure, may give rise to a variety of novel phases. Applying a magnetic field is an interesting and the easiest method to access these novel states.

An ideal kagome Heisenberg antiferromagnet suitable for the investigation of the spin-liquid state should have no structural distortions, no long-range magnetic interactions, very weak magnetic coupling between the kagome layers, a very low value of spin (preferably $S = 1/2$), and frustrated AFM exchange interactions. All of these ingredients enhance the quantum fluctuations and stabilize the spin-liquid state. Finding all these ingredients in a real kagome spin system is very challenging. Among the kagome systems reported thus far, there exists only one report on a pure metal-organic hybrid kagome compound with spin $S = 1/2$ on the vertices of kagome layers [11]. In our efforts to investigate novel magnetic states in a spin-$\frac{1}{2}$ kagome lattice with a nearest-neighbor (NN) AFM exchange interaction, some of us recently synthesized a $\{[Cu_3(CO_3)_2(bpe)_3]\cdot 2ClO_4\}_n$ [bpe=1,2-bis(4-pyridyl)ethane] compound, having a 3D metal-organic framework [12]. In this Rapid Communication, we report the results of magnetic susceptibility, specific heat, neutron depolarization, and neutron diffraction (ND) on this compound which show that strong quantum fluctuations enhanced by the geometrical frustration suppress the long-range magnetic ordering in $\{[Cu_3(CO_3)_2(bpe)_3]\cdot 2ClO_4\}_n$ [bpe=1,2-bis(4-pyridyl)ethane] down to at least 86 mK, the lowest temperature attained in our setup. The observed behavior points to a ground state with short-range canted AFM-type order. The proposed ground state is very fragile, and an applied field of 125 Oe (and higher) induces ferromagnetic (FM)-like correlations in this compound.

The polycrystalline sample was prepared by the solution method as mentioned in Ref. [12]. The x-ray diffraction study (Fig. S1 [13]) shows that the compound crystallizes in the

*Corresponding author: smyusuf@barc.gov.in

†Present address: Department of Chemistry, School of Chemical Sciences, Central University of Haryana, Jant-Pali, Mahendergarh 123 031, India.

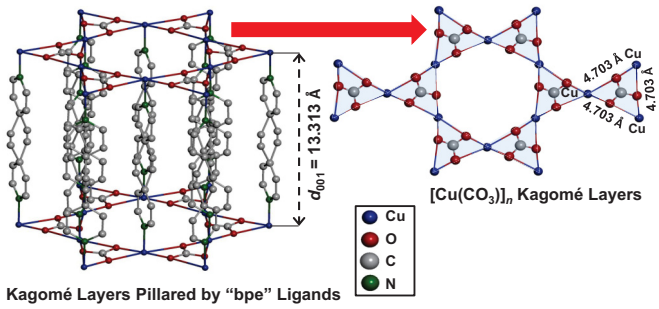

FIG. 1. Left: Schematic crystal structure of $\{[Cu_3(CO_3)_2(bpe)_3]\cdot 2ClO_4\}_n$ [bpe=1,2-bis(4-pyridyl)ethane] showing kagome layers pillared by the bpe linkers. For clarity, hydrogen atoms are not shown. Right: A 2D kagome layer viewed along the crystallographic c axis.

hexagonal structure (space group $P\bar{6}$ with $a = b = 9.314$ Å, $c = 13.313$ Å, $\alpha = \beta = 90°$, and $\gamma = 120°$). The crystal structure contains 2D kagome layers of Cu^{2+} and CO_3^{2-} in the crystallographic ab plane (Fig. 1). The $[Cu_3(CO_3)_2]^{2+}$ kagome layers are pillared by the bpe linkers along the crystallographic c axis. The x-ray diffraction measurements also confirm that the Cu^{2+} ions form a perfect kagome lattice with no structural distortions. The in-plane Cu-Cu distance is 4.703 Å and the out-of-plane Cu-Cu distance (the distance between the kagome layers) is ∼13.313 Å, which virtually ensures an ideal 2D character of the kagome layers with a negligible interlayer magnetic exchange interaction. The powder ND experiments were performed using the cold neutron powder diffractometer DMC ($\lambda = 2.44$ Å) at the Paul Scherrer Institute (PSI), Switzerland. The magnetic susceptibility measurements were carried out in a CRYOGENIC make vibrating sample magnetometer (VSM). The specific heat was measured using a Quantum Design physical property measurement system (PPMS).

Figure 2(a) depicts the static magnetic susceptibility (χ_{dc}) measured under $H = 100$ Oe. The χ_{dc} does not show any anomaly down to the lowest measured temperature of 3 K. High-temperature inverse magnetic susceptibility (above 150 K), shown in the inset of Fig. 2(a), after subtraction of a temperature-independent susceptibility $\chi_0 = 0.001\,95$ emu/mol Oe, follows the Curie-Weiss (CW) law with a negative value of the paramagnetic (PM) Curie temperature $\theta_{CW} \sim -2.9 \pm 0.9$ K and an effective paramagnetic moment (μ_{eff}) of $2.11 \pm 0.15\mu_B$/Cu [14]. The observed value of the μ_{eff} is higher than the theoretically expected value of $1.73\mu_B$ for Cu^{2+} ($S = 1/2$), assuming a pure electron value of the Landé g-factor. The observed higher value of μ_{eff} could be due to the higher value of the g-factors arising from the second-order contribution of the spin-orbit interaction. No bifurcation between field-cooled (FC) and zero-field-cooled (ZFC) magnetization is observed down to 4 K (Fig. S2).

In order to investigate further any possible presence of a long-range magnetic ordering (LRO), we have measured the ac magnetic susceptibility under a superimposed dc magnetic field [Figs. 2(b) and 2(c)]. At lower applied field (up to 100

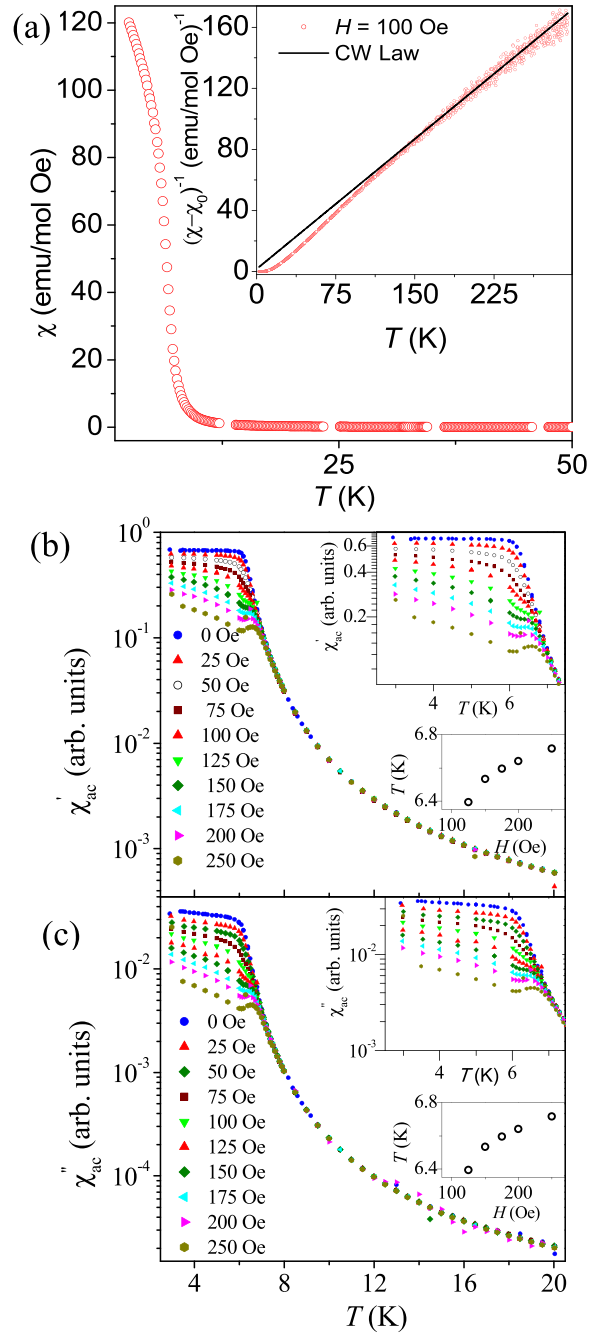

FIG. 2. (a) The temperature dependence of χ_{dc} measured with $H = 100$ Oe. Inset: Temperature dependence of reciprocal susceptibility after subtraction of a temperature-independent term χ_0. The open circles represent $\frac{1}{\chi_{dc}-\chi_0}$. The solid line represents the CW fit. (b) and (c) show the temperature dependences of χ'_{ac} and χ''_{ac}, respectively, measured at 987 Hz (with an ac field amplitude of 5 Oe) under various superimposed dc magnetic fields (FC condition). In zero field, no peak in the susceptibility has been observed. A broad peak at ∼6.5 K has been observed for fields higher than 125 Oe. Upper insets of (b) and (c): Zoomed-in view of (b) χ'_{ac} and (c) χ''_{ac} at low temperatures. Lower insets of (b) and (c): Field variations of the center of the broad peak observed in (b) χ'_{ac} and (c) χ''_{ac}.

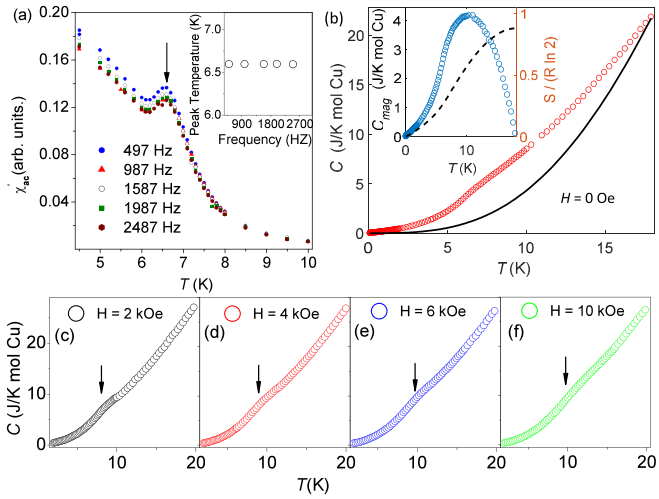

FIG. 3. (a) Temperature dependence of χ'_{ac} measured at varied frequencies under a superimposed dc magnetic field of 250 Oe. Inset of (a): Frequency dependence of the center of the broad peak observed in χ'_{ac}. (b)–(f) Temperature dependence of total specific heat, measured under various applied fields. Arrows mark the position of the anomaly. The solid line in (b) is the assumed lattice contribution (see Supplemental Material Fig. S5). Inset of (b): Extracted magnetic specific heat for zero-field data. The dashed line is the estimated magnetic entropy for zero field, normalized as a fraction of the total value $R \ln 2$ per Cu spin.

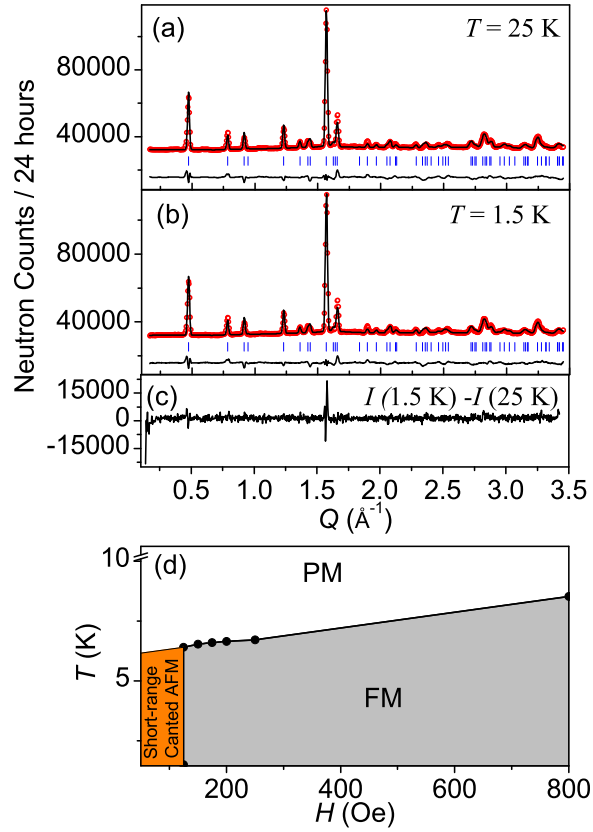

FIG. 4. Observed (open circles) and calculated (solid lines) ND patterns at (a) 25 K and (b) 1.5 K. The solid line at the bottom shows the difference between the observed and the calculated patterns. Vertical marks correspond to the positions of all allowed nuclear Bragg reflections. (c) Observed ND pattern at 1.5 K after subtraction of the nuclear pattern at 25 K. (d) Magnetic phase diagram derived from the thermodynamic and ND measurements.

Oe), the real part of ac susceptibility χ'_{ac} contains no signature of a LRO down to 2 K [Fig. 2(b)]. The imaginary part of ac susceptibility χ''_{ac} also increases with decreasing temperature, and contains no anomalies [Fig. 2(c)]. An applied field of 125 Oe induces a broad peak at ~6.5 K. The position of the peak shifts to higher temperatures with increasing magnetic field, and its amplitude decreases. No change in the peak position has been observed with a change in the frequency (under constant applied dc magnetic field) [Fig. 3(a)]. The observed peak indicates the presence of short-range spin correlations (SRSCs). The observed shift in peak position towards high temperature with increasing magnetic field [Figs. 2(b) and 2(c)] and no shift with frequency variation [Fig. 3(a)] confirm the FM nature of spin correlations under an applied magnetic field (for AFM correlations the peak should have shifted to lower temperatures [Figs. 2(b) and 2(c)] under increasing field). We also measured the frequency dependence of χ'_{ac} in zero applied magnetic field over the frequency range of 100–5000 Hz which shows a frequency-independent flattening behavior below ~6 K (Fig. S3), ruling out the presence of a spin glass state. The observed flattening of the real and imaginary parts of the ac susceptibility at low temperatures [Figs. 2(b) and 2(c)] could be due to a slowing down of the spin dynamics. The observed imaginary part of ac susceptibility indicates the presence of a weak ferromagnetic moment that arises due to a competition between the in-plane nearest-neighbor AFM and next-nearest-neighbor FM interactions as discussed later. We have also measured χ'_{ac} under different amplitudes of the driving ac field (under constant applied dc field H and frequency of the ac field), where no shift in the position of the broad peak (which appears above 125 Oe) has been observed with changing the amplitude of the driving ac field, ruling out the presence of magnetic domain wall pinning (Fig. S4).

The specific heat data provide further evidence for the absence of a LRO. In zero applied magnetic field, a minor anomaly (broad hump) in the specific heat is observed at ~6.5 K, however, no anomaly associated with a LRO is observed down to 86 mK [Fig. 3(b)]. The anomaly shifts to high temperatures with increasing the magnetic field [Figs. 3(b)–3(f)], consistent with the χ'_{ac} (under magnetic field) data [Figs. 2(b) and 2(c)]. The observed anomaly may arise due to the presence of SRSCs. The specific heat data from 86 mK to 18 K have been used to estimate the magnetic entropy. A lattice contribution to specific heat has been estimated from the Debye temperature of an isostructural nonmagnetic analog $\{[Cd_3(CO_3)_2(bpe)_3]\cdot 2ClO_4\}_n$ [bpe=1,2-bis(4-pyridyl)ethane] (see Supplemental Material Fig. S5). The magnetic entropy released in zero applied field below 18 K down to the lowest measured temperature of 86 mK was found to be 88% of $R \ln 2$ per mol of Cu spin. This indicates that if a LRO occurs at all below 86 mK, the maximum released entropy could be 12% of the total magnetic entropy, resulting in a highly reduced ordered moment for Cu^{2+}.

Figure 4 shows Rietveld-refined, using the FULLPROF program [15], powder ND patterns at $T = 25$ and 1.5 K in the absence of an external magnetic field. Neither additional magnetic Bragg peaks nor an enhancement in the intensity of the fundamental nuclear Bragg peaks has been observed down to 1.5 K (even after counting for 24 h at a fixed temperature), ruling out the presence of a LRO. All the observed patterns could be fitted by considering only the nuclear phase. Further, we carried out a neutron depolarization study [16] down to 3 K, where no depolarization of the neutron beam was observed, ruling out the presence of any FM or ferrimagnetic domains/clusters under an applied field of 50 Oe (Fig. S6 [13]).

We now turn our attention to the effect of an external magnetic field on spin-spin correlations and the magnetization. Since θ_{CW} represents the combined effect of all exchange interactions, the observed small negative value of the θ_{CW} in Fig. 2(a) indicates a close competition between AFM and FM exchange interactions, both having nearly similar values. At 1.5 K, the magnetization saturates ($\sim 3\mu_B$/f.u.) under $\sim$2 kOe (Fig. S7 [13]), which agrees with the theoretically expected value of $3\mu_B$/f.u. for a fully polarized FM state of the $S = \frac{1}{2}$ kagome lattice (with three Cu^{2+} spins per formula unit). In the literature, a quick saturation of the magnetization at $\mu_B B \sim J/20$ has been reported in a $S = 1/2$ metal-organic hybrid kagome antiferromagnet, which has been ascribed to the presence of competing AFM (intralayer) and FM (interlayer) interactions [11]. For the present system, besides the AFM interaction within the kagome layer, the presence of a FM interaction between kagome layers is also inferred from the observed data. Considering that the interkagome layer Cu-Cu distance is $\sim$3 times larger than the in-plane Cu-Cu distance, interkagome layer interactions are expected to be very small. The observed small negative value of the $\theta_{CW} \sim -2.9 \pm 0.9$ K is therefore closely related to a competition between the AFM and FM exchange interactions (both in plane). From the field-dependent magnetization, a technical saturation of magnetization, revealing a FM correlation, is evident up to $\sim$10 K (Fig. S7 [13]). The observed saturation in the magnetization arises due to a magnetic-field-induced FM-like state involving a possible weak interlayer FM exchange coupling and the presence of intralayer exchange interactions beyond the nearest neighbor [17] which could possibility play a significant role under external magnetic fields. In the ac susceptibility study [Figs. 2(b) and 2(c)], a magnetic-field-dependent shift of the observed broad peak to the higher temperature also indicates a field-induced ferromagneticlike transition. The magnetic phase diagram, derived from the thermodynamic and ND measurements, is drawn in Fig. 4(d). In the ac susceptibility study [Figs. 2(b) and 2(c)], a magnetic-field-dependent shift of the observed broad peak to the higher temperature also indicates a field-induced ferromagneticlike transition. The magnetic phase diagram, derived from the thermodynamic and ND measurements, is drawn in Fig. 4(d).

Now we compare the present results with those available in the literature for other spin $S = 1/2$ kagome systems, such as volborthite [18–21], herbertsmithite [22–25], kapellesite [26,27], vesignieite [28,29], and haydeeite [30], to gain further insight into the nature of spin-spin correlations. In volborthite $Cu_3V_2O_7(OH)_2 \cdot 2H_2O$, monoclinic structural distortion gives rise to anisotropic in-plane exchange interactions and the ND study shows no LRO down to millikelvin temperatures. For herbertsmithite $ZnCu_3(OH)_6Cl_2$, the thermodynamic and neutron scattering measurements show that though the CW temperature is 300 K, and no LRO is present down to 50 mK. In kapellasite, $ZnCu_3(OH)_6Cl_2$[26], a gapless spin-liquid behavior with dynamic SRSCs persisting down to 20 mK has been observed due to a competition between the FM (NN) and AFM (second- and third-neighbor) exchange interactions. In vesignieite, $BaCu_3V_2O_8(OH)_2$, magnetization and specific heat measurements show no signature of LRO despite a high value of $J_{AFM} \sim -53$ K. The mineral haydeeite, α-$MgCu_3(OD)_6Cl_2$, orders ferromagnetically below $T_c \sim 4.2$ K [30] due to the presence of both FM NN and AFM third-neighbor across-hexagon exchange interactions. For the structurally perfect metal-organic hybrid kagome compound Cu(1,3-bdc), NN Cu-Cu distances in the kagome plane and between the kagome layers are 4.5541 and 7.9716 Å, respectively. The exchange interaction in the kagome layer is AFM ($\theta_{CW} = -30$ K), however, it orders ferromagnetically at 2 K, due to the presence of a FM exchange interaction between kagome layers linked by the 1,3-bpc ligands [11,31]. The reported behavior indicates that the exchange interaction between kagome layers and in-plane second- and third-neighbor exchange interactions plays a very crucial role in stabilizing the various exotic states. For the present compound, the NN Cu-Cu distances in the kagome plane and between the kagome layers are 4.703 and 13.313 Å, respectively, suggesting a nearly 2D nature of the magnetic kagome lattice. The specific heat shows no signature of LRO down to 86 mK. The observed broad peak in the magnetic specific heat around 6.5 K indicates the presence of SRSCs. ND and neutron depolarization measurements combined with the specific heat measurements rule out the possibility of any LRO down to 86 mK. The observed behavior points to a ground state with quasistatic short-range canted AFM-type order with strong competing FM and AFM exchange interactions. Future experiments, preferably using single crystals, will be required to investigate the nature of the magnetic excitation (whether it is gapped or gapless) and to determine the effective low-energy Hamiltonian of the system, which will be helpful in understanding the proposed magnetic phase diagram. It would be interesting to investigate the presence of different exotic phases under external pressure. By replacing Cu^{2+} with other magnetic ions having small spin values, one can get other candidates for exotic quantum phases. By varying the distance and the overall angle between Cu^{2+} ions sitting on adjacent kagome layers, one can modify the FM interlayer exchange interaction and bring it close to a quantum critical point. Doping $\{[Cu_3(CO_3)_2(bpe)_3]\cdot 2ClO_4\}_n$ [bpe=1,2-bis(4-pyridyl)ethane] will be interesting to investigate emergent states of the quantum matter. Our findings pave the way for the further investigation of the quantum magnetism in metal-organic compounds.

In summary, our experimental results point to a lack of LRO in $\{[Cu_3(CO_3)_2(bpe)_3]\cdot 2ClO_4\}_n$ [bpe=1,2-bis(4-pyridyl)ethane] down to 86 mK. The ground state is fragile against external magnetic fields. The application of field (125 Oe and higher) induces FM spin-spin correlations, and

the magnetization saturates under a field of 2 kOe. The observed behavior has been ascribed to the presence of a field-induced interplane FM exchange interaction and intralayer exchange interactions beyond the nearest neighbor. The observed behavior is unique from those reported for the other kagome lattice antiferromagnets, as the present study indicates the crucial importance of interlayer FM interactions in tuning the magnetic properties of kagome Heisenberg antiferromagnets. The compound appears to be an ideal candidate for realizing the exotic ground state in a metal-organic compound, with spin-$\frac{1}{2}$ on a kagome lattice incorporating geometrical frustration and strong quantum fluctuations. The observed results in the present study may facilitate future studies to investigate the features of the proposed ground state with quasistatic short-range canted AFM-type spin correlations and especially how in-plane second-neighbor and interkagome layer interactions modify the generic magnetic phase diagram of kagome Heisenberg antiferromagnets involving quantum fluctuations.

ND experiments presented in this work were performed at the Swiss spallation neutron source SINQ, Paul Scherrer Institute, Villigen, Switzerland. The authors would like to acknowledge the help received from L. Keller in performing the ND experiments. The authors thank Dr. Ruta Kulkarni for help in performing the specific heat measurements. A.J. thanks Dr. M. D. Mukadam for his help during the specific heat measurements.

[1] L. Balents, Nature (London) **464**, 199 (2010).
[2] P. A. Lee, Science **321**, 1306 (2008).
[3] A. P. Ramirez, Annu. Rev. Mater. Sci. **24**, 453 (1994).
[4] J. E. Greedan, J. Mater. Chem. **11**, 37 (2001).
[5] A. Harrison, J. Phys.: Codens. Matter. **16**, S553 (2004).
[6] P. W. Anderson, Mater. Res. Bull. **8**, 153 (1973).
[7] M. Punk, D. Chowdhury, and S. Sachdev, Nat. Phys. **10**, 289 (2014).
[8] T. Han, J. S. Helton, S. Chu, D. G. Nocera, J. A. Rodriguez-Rivera, C. Broholm, and Y. S. Lee, Nature (London) **492**, 406 (2012).
[9] S. Depenbrock, I. P. McCulloch, and U. Schollwöck, Phys. Rev. Lett. **109**, 067201 (2012).
[10] S. Yan, D. A. Huse, and S. R. White, Science **332**, 1173 (2011).
[11] E. A. Nytko, J. S. Helton, P. Müller, and D. G. Nocera, J. Am. Chem. Soc. **130**, 2922 (2008).
[12] P. Kanoo, C. Madhu, G. Mostafa, T. K. Maji, A. Sundaresan, S. K. Pati, and C. N. R. Rao, Dalton Trans. **70**, 5062 (2009).
[13] See Supplemental Material at http://link.aps.org/supplemental/10.1103/PhysRevB.101.140413 for results of structural characterization (Fig. S1), temperature dependence of zero-field-cooled (ZFC) and field-cooled (FC) dc magnetization for $\{[Cu_3(CO_3)_2(bpe)_3]\cdot 2ClO_4\}_n$ [bpe=1,2-bis(4-pyridyl)ethane] (Fig. S2), temperature dependence of the χ'_{ac} measured at varied frequencies (Fig. S3), temperature dependence of the χ'_{ac} measured with varied amplitude of the probing ac field under a superimposed dc field of 250 Oe (Fig. S4), heat capacity versus temperature data for the magnetic sample $\{[Cu_3(CO_3)_2(bpe)_3]\cdot 2ClO_4\}_n$ [bpe=1,2-bis(4-pyridyl)ethane] and nonmagnetic analog $\{[Cd_3(CO_3)_2(bpe)_3]\cdot 2ClO_4\}_n$ [bpe=1,2-bis(4-pyridyl)ethane] (Fig. S5), temperature variation of the flipping ratio for the sample (Fig. S6), magnetization curves for the sample (Fig. S7), and temperature dependence of χ_{dc} measured under $H = 1000$ Oe for the nonmagnetic compound (Fig. S8).
[14] A. B. Harris, C. Kallin, and A. J. Berlinsky, Phys. Rev. B **45**, 2899 (1992).
[15] J. Rodríguez-Carvajal, Physica B **192**, 55 (1993).
[16] S. M. Yusuf and L. M. Rao, Pramana - J. Phys. **47**, 171 (1996).
[17] F. L. Buessen and S. Trebst, Phys. Rev. B **94**, 235138 (2016).
[18] Z. Hiroi, N. Kobayashi, M. Hanawa, M. Nohara, H. Takagi, Y. Kato, and M. Takigawa, J. Phys. Soc. Jpn. **70**, 3377 (2001).
[19] H. Yoshida, Y. Okamoto, T. Tayama, T. Sakakibara, M. Tokunaga, A. Matsuo, Y. Narumi, K. Kindo, M. Yoshida, M. Takigawa, and Z. Hiroi, J. Phys. Soc. Jpn. **78**, 043704 (2009).
[20] M. Yoshida, M. Takigawa, H. Yoshida, Y. Okamoto, and Z. Hiroi, Phys. Rev. Lett. **103**, 077207 (2009).
[21] Y. Okamoto, M. Tokunaga, H. Yoshida, A. Matsuo, K. Kindo, and Z. Hiroi, Phys. Rev. B **83**, 180407(R) (2011).
[22] M. P. Shores, E. A. Nytko, B. M. Bartlett, and D. G. Nocera, J. Am. Chem. Soc. **127**, 13462 (2005).
[23] M. Fe, T. Imai, T.-H. Han, and Y. S. Lee, Science **350**, 655 (2015).
[24] M. A. de Vries, J. R. Stewart, P. P. Deen, J. O. Piatek, G. J. Nilsen, H. M. Rønnow, and A. Harrison, Phys. Rev. Lett. **103**, 237201 (2009).
[25] M. Jeong, F. Bert, P. Mendels, F. Duc, J. C. Trombe, M. A. de Vries, and A. Harrison, Phys. Rev. Lett. **107**, 237201 (2011).
[26] R. H. Colman, C. Ritter, and A. S. Wills, Chem. Mater. **20**, 6897 (2008).
[27] B. Fåk, E. Kermarrec, L. Messio, B. Bernu, C. Lhuillier, F. Bert, P. Mendels, B. Koteswararao, F. Bouquet, J. Ollivier, A. D. Hillier, A. Amato, R. H. Colman, and A. S. Wills, Phys. Rev. Lett. **109**, 037208 (2012).
[28] Y. Okamoto, H. Yoshida, and Z. Hiroi, J. Phys. Soc. Jpn. **78**, 033701 (2009).
[29] W. Zhang, H. Ohta, S. Okubo, M. Fujisawa, T. Sakurai, Y. Okamoto, H. Yoshida, and Z. Hiro, J. Phys. Soc. Jpn. **79**, 023708 (2010).
[30] D. Boldrin, B. Fåk, M. Enderle, S. Bieri, J. Ollivier, S. Rols, P. Manuel, and A. S. Wills, Phys. Rev. B **91**, 220408(R) (2015).
[31] L. Marcipar, O. Ofer, A. Keren, E. A. Nytko, D. G. Nocera, Y. S. Lee, J. S. Helton, and C. Bains, Phys. Rev. B **80**, 132402 (2009).